Eur Biophys J (1985) 13: 45–58

European Biophysics Journal

Deconvolution of single photon counting data with a reference method and global analysis*

J.-E. Löfroth

Department of Physical Chemistry, Chalmers University of Technology and University of Göteborg, S-412 96 Göteborg, Sweden

Received November 29, 1984/Accepted May 21, 1985

Abstract. A method based on quenched references and global analysis was used to deconvolute time-resolved single photon counting data. The results from both computer simulated data and real experiments showed that highly accurate and reliable deconvolutions were possible. Fluorescence lifetimes and Stern-Volmer quenching constants for quenching with NaI were determined for the reference substances para-terphenyl, PPO (2,5-diphenyloxazol), POPOP (1,4-bis-(5-phenyl-2-oxazolyl)-benzene), and dimethyl-POPOP, all in ethanol. The fluorescence from a mixture of POPOP, anthracene, and diphenylanthracene in ethanol at different wavelengths was successfully resolved into the known relative contributions from the species at each wavelength. Fluorescence intensity decays of tryptophan in solution were studied at different wavelengths and globally analyzed with the method. Also, fluorescence anisotropy described by isotropic and anisotropic rotations in homogeneous and heterogeneous emitting systems were simulated and successfully deconvoluted. The method was applied to real fluorescence anisotropy data of diphenylanthracene and POPOP in paraffin oil, as well as to data from experiments on the blue copper-containing protein stellacyanin and its apo-form. In these cases, the method both corrected for errors due to, for example, the wavelength-dependent transit-times in the photomultiplier, and realized global deconvolutions of the total, parallel, and perpendicular components of the fluorescence. General algorithms for arbitrary fluorescence impulse responses are given.

Key words: Fluorescence, anisotropy, deconvolution, reference, global analysis

Introduction

Fluorescence decay data sampled with the single photon counting technique (Ware 1971; Knight and Selinger 1973) contain a number of errors. One of the major non-negligable experimental problems met with the technique, is due to the wavelength-dependent transit-time in the photomultiplier (Lewis et al. 1973; Wahl et al. 1974).

Let $F(t, em)$ be the observed fluorescence signal recorded at the emission wavelength and let $f(t)$ be the theoretical model used for the decay of the system under investigation, i.e., the fluorescence response of the system to a Dirac δ-excitation function. If further $L(t, \text{exc})$ is the time profile at the excitation wavelength of the actual pumping lamp, and $R(t, em)$ is the δ-pulse response of the electronic system at the emission wavelength, then

$$F(t, em) = I(t, \text{exc}, em) * f(t),$$

where $I(t, \text{exc}, em)$ is the instrument response function, which equals the convolution between $L(t, \text{exc})$ and $R(t, em)$: $I(t, \text{exc}, em) = L(t, \text{exc}) * R(t, em)$ (Ware 1971).

If $F(t, em)$ and $I(t, \text{exc}, em)$ are given, then $f(t)$ may be obtained with a variety of deconvolution methods (Knight and Selinger 1971; Helman 1971; Ware et al. 1973; Almgren 1974; Isenberg 1975; McKinnon et al. 1977; Valeur 1978). However, it is not possible to directly record $I(t, \text{exc}, em)$. If the fluorescent sample is replaced by a scattering solution, then $I(t, \text{exc}, \text{exc})$ $(= L(t, \text{exc}) * R(t, \text{exc}))$ and $I(t, em, em)$ $(= L(t, em) * R(t, em))$ may be obtained. ($R(t, \text{exc})$ is the δ-response of the electronic system at the excitation wavelength and $L(t, em)$ is the time profile of the exciting lamp at the emission wavelength.) In the first case the different time responses of the detection system, mainly the photomultiplier, at the excitation and emission wavelengths will disturb the analysis, $F(t, em)$

* A preliminary account of this work was presented at the NATO ASI in Acireale, Italy (Löfroth 1985a, in press)

being recorded at the emission wavelength while $I(t, \text{exc}, \text{exc})$ is recorded at the excitation wavelength. In the other situation different profiles of $L(t)$ at the excitation and emission wavelengths may introduce severe errors in the parameter estimation, the true $L(t)$ being at the excitation wavelength.

In the literature, different approaches to overcome the problem have been presented (Wahl et al. 1974; Wahl 1979; Isenberg 1975; Rayner et al. 1976, 1977; Gaudochon and Wahl 1978; Birch and Imhof 1982; Wijnaendts van Resandt et al. 1982; Libertini and Small 1984). Among these the use of references have been suggested. In this report one of the reference methods has been further developed to a method based on quenched references. Also, the advantages of global analysis have been considered. Global analysis has been applied in fluorescence anisotropy studies (Ehrenberg et al. 1979) and was recently given an exhaustive description as a method to simultaneously deconvolute observed decays (Knutson et al. 1983). If, for example, the fluorescence emanates from two differently emitting species and is recorded at different wavelengths, the observed decays should be described by two lifetimes with different weights at each wavelength. In a global analysis of these kinds of systems all of the decay curves are deconvoluted at the same time with the constraint that the analysis should give only two lifetimes. Evidently, it is critical for a correct analysis that the wavelength-dependent transit-time problems have been taken care of. So far, only the shift method has been applied together with gobal analysis, and in most applications the shift method is only a first-order correction, as discussed by Ware et al. (Ware et al. 1983 and references therein).

Thus, in this work we present a method based on quenched references and global analysis of fluorescence intensity and anisotropy decay data. The alogrithms given here for the method are applicable to data sampled with the single photon counting technique, but the ideas are easily applied to experiments in connection with the phase and modulation technique. The method has been used during the past two years in our laboratory and has so far proved to be reliable and convenient to use in all experimental situations. In this paper both computer generated data and data from experiments on real systems are presented and analyzed with the method, which we call the global-reference deconvolution method.

Theory

The algorithms presented below are based on the assumption that the fluorescence decays and the fluorescence anisotropies are each described by a sum of exponentials. However, general algorithms for arbitrary decays are given in the Appendix.

A. General

Let $f(t) = \Sigma\, a_i \exp(-k_i t)$ where $k_i = 1/\tau_i =$ the reciprocal lifetime of species "i". Further let $f_r(t) = \exp(-k_r t)$, where $k_r = 1/\tau_r =$ the reciprocal lifetime of the reference compound. The observed fluorescence of the reference is denoted $F_r(t)$ and is excited and observed at the same wavelengths as $F(t)$. Then

$$F(t, em) = I(t, \text{exc}, em) * f(t) \tag{1}$$

and

$$F_r(t, em) = I(t, \text{exc}, em) * f_r(t)\,. \tag{2}$$

Taking the Laplace transforms, denoted $L(\,)$, of Eqs. (1) and (2) gives after division

$$L(F) = L(F_r)\,\frac{L(f)}{L(f_r)} = L(F_r)\,(s + k_r)\,\Sigma\frac{a_i}{s + k_i}$$

$$= L(F_r)\,\Sigma\, a_i + L(F_r)\,L\{\Sigma\, a_i(k_r - k_i)\exp(-k_i t)\}\,,$$

where s is the Laplace parameter and the dependence on wavelength has been omitted for clarity. Using the convolution theorem again gives

$$F(t, em) = F_r(t, em)\,\Sigma\, a_i + F_r(t, em) * \{\Sigma\, a_i(k_r - k_i)\exp(-k_i(t))\}\,. \tag{3a}$$

By varying k_r, e.g., by quenching, and/or a_i, e.g., by experiments at different excitation and/or emission wavelengths, the different experiments, j, *simultaneously* should fulfil

$$F^{(j)}(t) = F_r^{(j)}(t)\,\Sigma\, a_i^{(j)} + F_r^{(j)}(t) * \{\Sigma\, a_i^{(j)}(k_r^{(j)} - k_i)\exp(-k_i t)\}\,. \tag{3b}$$

Given the $2j$ observed decays $F^{(j)}(t)$ and $F_r^{(j)}(t)$, the photophysics of $f(t)$, i.e., $a_i^{(j)}$ and k_i can be obtained, e.g., by non-linear least-squares fitting of the right hand side of Eq. (3b) to $F^{(j)}(t)$. The procedure is described and discussed more in detail in the Data analysis section below. It is pertinent to emphasize that the $k_r^{(j)}$ during the analyses do not need to be known, but that instead they too may be estimated. It emerged that it is in fact an advantage not to fix $k_r^{(j)}$ during the analysis, as will be discussed below in the Discussion section. Also, it is noteworthy that (3a) closely resembles the algorithm which was proposed and utilized when excimer emission was deconvoluted with the monomer emission from the same system (Almgren 1974; Lakowicz and Balter 1982).

B. Fluorescence anisotropy

In fluorescence anisotropy experiments the fluorescence is normally excited with vertically linearly polarized light while different polarized components of the emission are recorded. Mostly the two components parallel (f_{pa}) and perpendicular (f_{pe}) to the vertical are followed and the anisotropy computed according to:

$$r(t) = \frac{f_{pa}(t) - f_{pe}(t)}{f_{pa}(t) + 2 f_{pe}(t)}, \tag{4}$$

where the components are assumed to have been normalized with respect to each other. However, $r(t)$ cannot be obtained as

$$r(t) = \frac{F_{pa}(t) - F_{pe}(t)}{F_{pa}(t) + 2 F_{pe}(t)} \tag{5}$$

unless $I(t)$ is a true δ-pulse, which means that (5) must be rearranged when deconvolution is necessary. This might be done in several ways. The most attractive would seem to be to use the fact the denominator of (4) represents the total fluorescence, $f_{55}(t)$, where the subscript "55" indicates that the normalized component of the fluorescence has been obtained with the analyzer set at 54.74° to the vertical. Rearrangement of (4) then gives

$$f_{pa}(t) = \tfrac{2}{3} r(t) f_{55}(t) + \tfrac{1}{3} f_{55}(t) \tag{6}$$

and

$$f_{pe}(t) = \tfrac{1}{3} f_{55}(t) - \tfrac{1}{3} r(t) f_{55}(t) \tag{7}$$

or

$$F_{pa}(t) = \tfrac{2}{3} I_{pa}(t) * (r(t) f_{55}(t)) + \tfrac{1}{3} I_{pa}(t) * f_{55}(t) \tag{8}$$

and

$$F_{pe}(t) = \tfrac{1}{3} I_{pe}(t) * f_{55}(t) - \tfrac{1}{3} I_{pe}(t) * (r(t) f_{55}(t)). \tag{9}$$

If we assume that the response function $R(t, em)$ does not show any dependence in time on the state of polarization of the incident photons, Laplace transformation and the inverse transformations of (2), (8), and (9) gives, with the same procedure as earlier

$$\begin{aligned} F_{pa}(t) &= \tfrac{2}{3} F^{pa}_{r,55}(t) \Sigma\Sigma r_n a_i \\ &+ \tfrac{2}{3} F^{pa}_{r,55}(t) * \Sigma\{\Sigma r_n a_i (k_r - k_n - k_i) \exp(-(k_n + k_i) t)\} \\ &+ \tfrac{1}{3} F^{pa}_{r,55}(t) \Sigma a_i + \tfrac{1}{3} F^{pa}_{r,55}(t) * \{\Sigma a_i (k_r - k_i) \exp(-k_i t)\} \end{aligned} \tag{10a}$$

and

$$\begin{aligned} F_{pe}(t) &= \tfrac{1}{3} F^{pe}_{r,55}(t) \Sigma a_i \\ &+ \tfrac{1}{3} F^{pe}_{r,55}(t) * \{\Sigma a_i (k_r - k_i) \exp(-k_i t)\} \\ &- \tfrac{1}{3} F^{pe}_{r,55}(t) \Sigma\Sigma r_n a_i \\ &- \tfrac{1}{3} F^{pe}_{r,55}(t) * \Sigma\{\Sigma r_n a_i (k_r - k_n - k_i) \exp(-(k_n + k_i) t)\} \end{aligned} \tag{10b}$$

where it has been assumed that $r(t) = \Sigma r_n \exp(-k_n t)$, $k_n = 1/\Phi_n$ = the reciprocal of the rotational correlation time, Φ_n. The superscripts "pa" and "pe" on $F_{r,55}(t)$ indicate that $F_{r,55}(t)$ was concurrently recorded with the fluorescence signal denoted by the superscript. For $F_{55}(t)$ Eq. (3a) applies, with the superscript "55" on $F_{r,55}(t)$.

It is seen that $F_{55}(t)$, $F_{pa}(t)$, and $F_{pe}(t)$ contain common information. Thus, a global analysis should give as output the common parameters, i.e., a_i, r_n, k_i, k_n, and k_r, when the three curves are analyzed at the same time. These ideas, however only applied to $F_{pa}(t)$ and $F_{pe}(t)$ and with the shift method, were discussed some years ago (Gilbert 1983), and had earlier been applied to $F_{55}(t)$ and $F_{pa}(t)$ (Ehrenberg et al. 1979). Also, different experiments, j, should be done, in which the values of k_r are varied by quenching and, particularly, values of the r_n can be varied by experiments at different excitation wavelengths, the r_n's for any studied system being functions of the excitation wavelength. Thus the experiments give $F^{(j)}_{55}(t)$, $F^{(j)}_{pa}(t)$, $F^{(j)}_{pe}(t)$, and $F^{(j)}_{r,55}(t)$ which are linked not only by the parameters $a^{(j)}_i$, $r^{(j)}_n$, $k^{(j)}_r$, k_i and k_n within each experiment but also from one experiment to another by k_i and k_n. However, it must be emphasized that an unfortunately chosen degree of quenching of the reference might cancel one of the exponentials in Eqs. (10a) and (10b). Therefore, again, it is highly desirable to carry out the experiments with at least two differently quenched references. Also, during the analysis it is advisable to estimate the reference lifetimes, as discussed below in the Experimental section.

Data analysis

In this work deconvolutions have been carried out with an iterative procedure (McKinnon et al. 1977). Thus the right hand side of Eqs. (3b), (10a), and (10b) were fitted with a non-linear least-squares procedure to the observed curves. The convolutions which were necessary were carried out using the fast convolution algorithm (Grinvald and Steinberg 1974). The computer program was based on a modified Levenberg-Marquardt algorithm available from IMSL, Texas, USA (subroutine ZXSSQ, International Mathematical and Statistical Libraries, Houston, Texas). This subroutine does not need any specified derivatives and therefore it was conveniently fast to use in connection with global analysis.

Both the computer-generated decays and the data from the real experiments were deconvoluted using the whole curve of the reference while the fitting range was chosen to start and stop in the channels with approximately 100 counts. The re-

duced χ^2-test (χ^2_v), the z-value from the runs' test, and the weighted residual (WRES) plots were used to judge the quality of the fits. Standard deviations of estimated parameters were calculated from the curvature of χ^2_v in the region of the best fit. The statistical accuracy of estimates of non-linear least squares fits have been discussed in detail elsewhere (Wahl 1977; Selinger and Hinde 1983). When more than one decay was deconvoluted in a global analysis, the best simultaneous fit to all decays was assumed to have been obtained when the total sum of the weighted squared residuals had a minimum, i.e., when a minimum was found in

$$SSQ = \sum_{i=1}^{N1} \sum_{j=1}^{N2} (\mathrm{WRES}^{(j)}(i))^2,$$

where

$$\mathrm{WRES}^{(j)}(i) = \frac{F^{o(j)}(i) - F^{c(j)}(i)}{(F^{o(j)}(i))^{1/2}},$$

and where $F^{o(j)}(i)$ and $F^{c(j)}(i)$ were the observed and, in each iteration, calculated fluorescence in channel "i" of experiment "j". $N1$ was the number of channels used in the fitting procedure and $N2$ was the number of experimental curves to be deconvoluted. For fluorescence anisotropy analysis the total sum which was minimized was obtained as

$$SSQ = SSQ_{55} + SSQ_{\mathrm{pa}} + SSQ_{\mathrm{pe}},$$

where

$$SSQ_{55} = \sum_{i=1}^{N1} \sum_{j=1}^{N2} (\mathrm{WRES}_{55}^{(j)}(i))^2$$

$$\mathrm{WRES}_{55}^{(j)}(i) = \frac{F_{55}^{o(j)}(i) - F_{55}^{c(j)}(i)}{(F_{55}^{o(j)}(i))^{1/2}}$$

and similarly for SSQ_{pa} and SSQ_{pe}. Once the minimum of SSQ was found, the individual χ^2_v and z-values were calculated from the curves of $\mathrm{WRES}^{(j)}(i)$, which also gave the WRES-plots for the individual curves. This global analysis is a somewhat modified version of the one presented earlier (Knutson et al. 1983). Also, the appropriate weighting factor in the denominator of $\mathrm{WRES}^{(j)}(i)$ has recently been suggested to be of a more complicated form:

$$(F^{o(j)}(i) + f(0)\, F_r^{(j)}(i))^{1/2},$$

which however has not yet been tested in our laboratory (Zuker et al., in press).

When $F_{55}(t)$, $F_{\mathrm{pa}}(t)$, and $F_{\mathrm{pe}}(t)$ were globally analyzed, the normalisation of the curves with respect to each other was carried out *during* the deconvolution. The $F_{55}(t)$ curve was regarded as already normalized. The estimates of a_i belonging to $F^c_{\mathrm{pa}}(t)$ were then multiplied, in each iteration, by the factor

$$\frac{3}{1+2\langle r\rangle} \frac{\int F_{\mathrm{pa}}(t)\,\mathrm{d}t}{\int F_{55}(t)\,\mathrm{d}t} \frac{\int F_{r,55}^{55}(t)\,\mathrm{d}t}{\int F_{r,55}^{\mathrm{pa}}(t)\,\mathrm{d}t} \qquad (11\,\mathrm{a})$$

while the estimates of a_i belonging to $F^c_{\mathrm{pe}}(t)$ were multiplied by

$$\frac{3}{1-\langle r\rangle} \frac{\int F_{\mathrm{pe}}(t)\,\mathrm{d}t}{\int F_{55}(t)\,\mathrm{d}t} \frac{\int F_{r,55}^{55}(t)\,\mathrm{d}t}{\int F_{r,55}^{\mathrm{pe}}(t)\,\mathrm{d}t}. \qquad (11\,\mathrm{b})$$

The integrals in Eqs. (11a) and (11b) were calculated from the total number of counts collected in the decays. In this way the statistics of $F_{55}(t)$, $F_{\mathrm{pa}}(t)$, and $F_{\mathrm{pe}}(t)$ were preserved in the simplest proper weighting of the residuals possible for the minimization. A cut-off error in the integrals can be a problem in analysis if the fluorescence signals decay slowly with respect to the anisotropy, but was not so in the present study. Otherwise, a Laplace transformation of the data is suggested to extrapolate the signals to infinity (Almgren 1974). The steady state anisotropy, $\langle r\rangle$, of Eqs. (11a) and (11b) was determined as described in the Experimental section.

Experimental

A. Computer generated data

Single-photon-counting data were simulated by computer to critically test the method. A realistic $I(t)$ was obtained by recording scattered light from a $H_2(g)$ flashlamp in 2,048 channels with 43 ps channel^{-1} with the instrument described below. Fluorescence decays, $F(t)$, were obtained by convoluting $I(t)$ with different models to give $F_{55}(t)$, $F_{r,55}^{55}(t)$, $F_{r,55}^{\mathrm{pa}}(t)$, $F_{r,55}^{\mathrm{pe}}(t)$ (all according to Eqs. (1) and (2)), $F_{\mathrm{pa}}(t)$ and $F_{\mathrm{pe}}(t)$ (Eq. (8) and Eq. (9) respectively). The choice of parameters describing $f_{55}(t)$ and $r(t)$ was in many cases dictated by results which have been reported for real systems, while k_r values were chosen to approximately span the range corresponding to k_r values for the references used in this study. The cross terms in the product $r(t) f_{55}(t)$ in Eqs. (8) and (9) were excluded in some generated $F_{\mathrm{pa}}(t)$ and $F_{\mathrm{pe}}(t)$ curves. The steady state anisotropy, which is needed for normalization, Eqs. (11a) and (11b), was calculated as $\langle r\rangle = \int r(t) f_{55}(t)\,\mathrm{d}t / \int f_{55}(t)\,\mathrm{d}t$. In order to have the decays non-normalized, which would be the case in real experiments, different values of Σa_i in Eqs. (1), (8), and (9) were used when $F_{55}(t)$, $F_{\mathrm{pa}}(t)$, and $F_{\mathrm{pe}}(t)$ were simulated. Also, the $F_{r,55}(t)$ curves were scaled to different heights. The number of counts at the top of the curves varied from 10^4 to 10^5. Finally, $G(t)(F(t))^{1/2}$ was added to each value of $F(t)$ to mimic Poissonian noise. $G(t)$ for each channel was

Table 1. Computer simulated $F_{55}(t)$ decays and results from deconvolutions with various references. All times are given in nanoseconds

Generated $F_{55}(t)$				Results from deconvolutions				
a_i	τ_i	[a]	τ_r	$a_{i,\text{out}}$	$\tau_{i,\text{out}}$	$\tau_{r,\text{out}}$	χ^2_ν	z
1.000	2.00	1	0.25	1.000 ± 0.015	1.99 ± 0.02	0.23 ± 0.01	0.85	0.33
			5.00	1.000 ± 0.015	1.99 ± 0.02	4.97 ± 0.04	10.0	1.45
1.000	5.00	2	0.25	1.000 ± 0.016	4.99 ± 0.06	0.23 ± 0.01	0.70	0.33
			2.00	1.000 ± 0.016	4.99 ± 0.06	1.99 ± 0.03	0.79	0.53
0.600	2.00	3	0.25	0.611 ± 0.020	1.98 ± 0.06	0.23 ± 0.01	1.14	0.32
0.400	5.00			0.389 ± 0.008	5.03 ± 0.07			
			0.50	0.606 ± 0.022	1.95 ± 0.07	0.48 ± 0.01	0.70	0.58
				0.394 ± 0.009	4.99 ± 0.08			
			5.00	1.000 ± 0.016	2.00 ± 0.03	3.13 ± 0.04	2.86	0.14
			5.00	0.994 ± 0.015	2.01 ± 0.03	3.17 ± 0.03	2.93	0.17
				0.006 ± 0.007	4.14 ± 3.32			
0.700	0.60	4	0.25	0.705 ± 0.004	0.60 ± 0.02	0.22 ± 0.01	0.91	0.45
0.300	3.50			0.295 ± 0.001	3.51 ± 0.03			
0.600	0.60	5	0.25	1.000 ± 0.015	3.41 ± 0.04	0.80 ± 0.01	35.2	8.13
0.380	3.00		0.25	0.840 ± 0.018	2.09 ± 0.04	0.48 ± 0.01	3.25	5.13
0.020	9.00			0.160 ± 0.006	5.54 ± 0.13			
			0.25	0.674 ± 0.034	0.45 ± 0.03	0.14 ± 0.01	0.94	0.11
				0.305 ± 0.007	2.90 ± 0.05			
				0.021 ± 0.002	8.20 ± 0.43			
			0.25	0.602 ± 0.032	0.65 ± 0.04			
				0.378 ± 0.008	3.04 ± 0.05	0.23 (fix)	0.99	0.53
				0.020 ± 0.002	9.04 ± 0.53			
1.000	1.25		0.22	1.000 ± 0.017	1.24 ± 0.02	0.22 ± 0.01	1.12	1.34
			[b]	1.000 ± 0.018	1.24 ± 0.04	0.18 ± 0.01	1.17	0.66
0.800	1.25		0.22	0.807 ± 0.029	1.19 ± 0.04	0.18 ± 0.01	1.01	0.12
0.200	5.00			0.193 ± 0.007	4.89 ± 0.12			
			0.22	0.807 ± 0.029	1.29 ± 0.05	0.22[c]	1.12	0.48
				0.193 ± 0.007	5.00 ± 0.13			
			[b]	0.807 ± 0.029	1.18 ± 0.04	0.14	1.01	0.12
				0.193 ± 0.007	4.88 ± 0.12			
			[b]	0.807 ± 0.029	1.28 ± 0.05	0.18[c]	1.13	0.60
				0.193 ± 0.007	4.99 ± 0.13			

[a] The number given is referred to in Table 2

[b] The reference decay was simulated as $I(t) * \exp(-at)\exp(-b\sqrt{t})$, where $a = 4.47\ \text{ns}^{-1}$ and $b = 0.644\ \text{ns}^{-1/2}$ to mimic a transient term. See also the discussion in the Results section, B:Real experiments

[c] The result was obtained when k_r was fixed at the value estimated in the preceding deconvolution of the curve $\exp(-t/1.25)$

chosen at random by a number generator (IMSL subroutine GGNML) from a Gaussian distribution with a mean of zero and a standard deviation of one. This procedure has proved to be accurate in other simulation experiments (Almgren and Löfroth 1982). Some of the simulated curves are given in Tables 1 and 2 and one generated set of anisotropy decays is shown in Fig. 1. In the final deconvolutions only every eighth channel was used of the simulated data, giving a time division, 0.344 ns channel^{-1}, comparable to what was used in the real experiments.

B. Materials

PTP (para-terphenyl, Eastman, puriss.), PPO (2,5-diphenyloxazole, Fluka, puriss.), POPOP (1,4-bis-(5-phenyl-2-oxazolyl)-benzene, Fluka, puriss.), DIMPOPOP (1,4-bis-(4-methyl-5-phenyl-2-oxazolyl)-benzene, Fluka, puriss.), anthracene (Merck, p.a.), DPA (9,10-diphenylanthracene, ICN), and NaI (Merck, p.a.) were used as supplied. Trp (L-tryptophan, Sigma) was twice recrystallized from water. SC (stellacyanin, apo- and holoforms) were prepared as described elsewhere (Reinhammar 1970; Dahlin et al. 1984).

Solutions were made of PTP, PPO, POPOP, DIMPOPOP, anthracene, and DPA in ethanol (99%) to give suitable absorbances ($A_{1\,\text{cm}} = 0.05$ to 0.20) at the excitation wavelength (295 nm for PTP and PPO, 356 nm for the others). A mixture of POPOP, anthracene, and DPA was obtained from these solutions by mixing appropriate known volumes. Trp was dissolved in a potassium phosphate buffer

Table 2. Computer simulated fluorescence anisotropy decays and results from deconvolutions with a reference with $1/k_r = 0.25$ ns (expected). All times are given in nanoseconds

Generated decays				Results from deconvolutions								
r_n	θ_n	$\langle r \rangle$	[a]	r_n	θ_n	[b] a_i	[b] τ_i	[b] τ_r	χ^2_{v55}	z_{55}	χ^2_{vpa}	z_{pa}
0.180	10.00	0.120	1	0.185 ± 0.016	9.55 ± 2.42	1.000	4.99	0.23	0.72	0.25	1.12	0.83
0.200	0.88	0.230	2	0.212 ± 0.055	0.85 ± 0.31	1.000	4.98	0.23	0.72	0.13	1.20	0.92
0.200	∞			0.199 ± 0.013	–							
0.130	0.70	0.038	3	0.139 ± 0.044	0.69 ± 0.36	0.611	1.99	0.22	1.15	0.00	0.97	0.19[d]
0.070	7.00	[c]		0.029 ± 0.008	22.2 ± 36.7	0.389	5.01					
			3	0.085 ± 0.029	0.58 ± 0.29	0.607	1.96	0.22	1.14	0.06	0.96	0.22[e]
				0.031 ± 0.008	18.2 ± 24.9	0.393	4.99					
		0.069	3	0.181 ± 0.030	0.73 ± 0.18	0.611	1.94	0.21	1.15	0.23	1.28	1.75[d]
		[f]		0.105 ± 0.021	6.01 ± 2.32	0.389	5.00					
			3	0.164 ± 0.029	0.69 ± 0.19	0.612	1.96	0.21	1.17	0.06	1.34	1.76[e]
				0.054 ± 0.010	9.65 ± 5.81	0.388	5.00					
0.150	3.00	0.096	3	0.103 ± 0.015	1.93 ± 0.56	0.606	2.00	0.23	1.10	0.02	1.39	0.62[d]
0.150	10.00	[c]		0.141 ± 0.017	10.9 ± 3.46	0.394	5.00	(fix)				
		0.178	3	0.173 ± 0.016	2.83 ± 0.55	0.610	2.01	0.23	1.08	0.32	1.56	0.58[e]
		[f]		0.133 ± 0.011	11.8 ± 3.29	0.390	5.02	(fix)				
0.100	1.00	0.114	4	0.093 ± 0.028	0.83 ± 0.45	0.705	0.60	0.22	0.91	0.45	0.89	0.42[e,g]
0.100	10.00	[f]		0.107 ± 0.012	9.52 ± 3.95	0.295	3.51					
0.200	3.00	0.109	5	0.202 ± 0.018	2.83 ± 0.67	0.636	0.58	0.20	1.05	0.97	1.19	0.39
						0.351	3.11					
						0.012	10.6					
			5	0.204 ± 0.020	2.82 ± 0.68	0.609	0.63	0.23	1.06	0.97	1.22	0.58
						0.379	3.08	(fix)				
						0.015	10.1					

[a] The number refers to the $F_{55}(t)$ decay of Table 1 which was used in the simulations
[b] The standard deviations of these estimates were of the order reported in Table 1
[c] The crossterms in $r(t) f_{55}(t)$ were excluded in the simulations
[d] The crossterms were excluded in the analysis
[e] The crossterms were included in the analysis
[f] The crossterms were included in the simulations
[g] The χ^2_v and z for $F_{pe}(t)$ were 0.97 and 0.48 respectively. This decay is illustrated in Fig. 1

solution (0.1 *M*, pH = 7.1 at 20 °C) to give an absorbance of $A_{1\,cm} = 0.5$ at 295 nm. The same buffer was used to prepare the SC solutions ($A_{1\,cm} = 0.45$ at 295 nm). A series of reference solutions with different concentrations of NaI was made from stock solutions of PTP, PPO, POPOP, and DIMPOPOP in ethanol. The concentration of NaI varied from 0 *M* to 0.85 *M*. For the fluorescence anisotropy experiments, POPOP and DPA were dissolved in paraffin oil (Fluka, IR). The solutions were not degassed and the temperature was kept at 20 °C in all measurements. Fresh solutions were always prepared for each experiment and the NaI solutions were prepared and kept in the dark as much as possible.

C. Instrumental

The single-photon-counting instrument used in this study has been described in detail elsewhere (Löfroth 1982). Briefly, the samples were excited with a nanosecond thyratron-gated flashlamp (Edinburgh Instruments Ltd, model 199F) run at 26 kHz in $N_2(g)$ at 0.5 atm. The excitation and emission wavelengths were chosen with monochromators from Jobin-Yvon (H10UV and H10VIS respectively), except for the anisotropy experiments on SC. In these cases a 369 nm interference filter (FWHM 13 nm) was used to select the emission. The slits of the monochromators were set to give 16 nm FWHM. A Glan prism polarizer was set at 0° to the vertical in the excitation beam, while either the 55°, 0°, or 90° components were selected in the emission beam by a film polarizer (Polaroid HNP'B). The emission was measured with a Hamamatsu R928 photomultiplier with a modified Hamamatsu base. The counting rate at the anode was kept below 500 Hz and the resolution of the multichannel analyzer was set at 0.345 ns channel^{-1}. 10^4 counts were normally col-

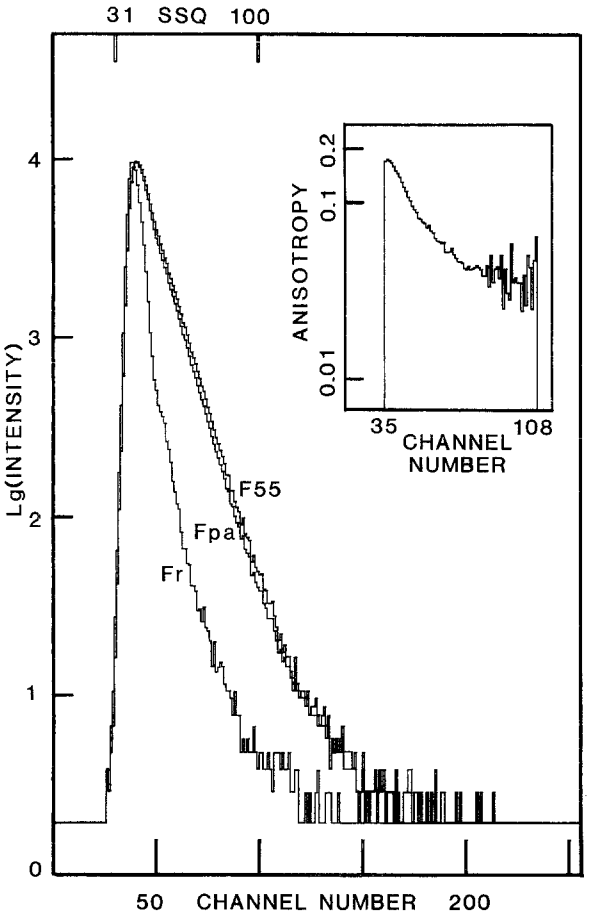

Fig. 1. Computer simulated decays for fluorescence anisotropy deconvolutions. $F_{55}(t)$, $F_{pa}(t)$, $F_{pe}(t)$ (not shown for the sake of clearness), and $F_r(t)$ were simulated from

$f_{55}(t) = 0.70 \exp(-t/0.60\text{ ns}) + 0.30 \exp(-t/3.5\text{ ns})$,

$r(t) = 0.10 \exp(-t/1.0\text{ ns}) + 0.10 \exp(-t/10.0\text{ ns})$

and

$f_r(t) = \exp(-t/0.25\text{ ns})$.

The crossterms were included. The decays have been normalized to 10^4 counts in their maxima. Time-division: 0.344 ns channel^{-1}. Insert: the "pseudo-anisotropy" calculated from simulated curves as $r(t) = (F_{pa}(t) - F_{pe}(t))/F_{55}(t)$

lected at the peak of the $F_{55}(t)$ curves and 2×10^4 counts for the $F^{55}_{r,55}(t)$ decays. $F_{pa}(t)$ and $F_{pe}(t)$ generally contained 2×10^4 counts at their maxima, while $F^{pa}_{r,55}(t)$ and $F^{pe}_{r,55}(t)$ contained $3 \times 10^4 - 5 \times 10^4$. The reference decay curves were recorded concurrently with the respective sample decay. The steady-state anisotropy, $\langle r \rangle$, was measured with the same instrumental setup, but the flashlamp was replaced by a steady-state tungsten or deuterium lamp. $\langle r \rangle$ was calculated as $(R-1)/(R+2)$ where $R = VV \cdot HH/VH/HV$ where, for example, HV was the number of photon events counted at the anode when the sample was excited with the polarizer at 90° to the vertical and the analyzer set at 0° to the vertical. *VV, HV, VH,* and *HH* were registered alternately during typically 10 s each in several cycles to minimize errors due to drift in the steady-state lamp.

Results and discussions

The results of this study will be discussed in two parts. First the results from the computer generated experiments are presented. The conclusions which are drawn and the experience gained will then form a platform for the analysis of real experiments. The aim of this paper is to present the investigation technique and not to present detailed discussions on the physical and chemical behaviour of the systems studied. Those will be presented elsewhere.

A. Computer generated data

The results of deconvolutions of different $F_{55}(t)$ curves with different reference decays are given in Table 1, and confirm that the reference method worked well in most cases for these kinds of data. The estimated parameters a_i, $1/k_i$ and $1/k_r$ were in excellent agreement with the expected values. Also, the χ^2_v and z-values were acceptable for the number of degrees of freedom (approximately 90) at a level of 5% significance ($0.77 < \chi^2_v < 1.26$, $|z| < 1.9$).

Several important conclusions were drawn. The statistical tests indicated better fits when fast reference decays were used in the deconvolutions. Short reference lifetimes could be estimated with Eq. (3b) with high accuracy when fluorescence signals described by single exponentials were analyzed. The limiting factor seemed to be the time-division, which should be of the order of $1/k_r$ or less, as discused below. In cases when complicated fluorescence decays (more than one exponential in $f(t)$) were analyzed the true number of exponentials were more accurately and reliably found when deconvolutions were carried out with references with different k_r, as this approach made it possible to put different weights to the contribution from an exponential, (Eq. (3b)). Also, the estimated value of k_r seemed to indicate if the fit was acceptable or not. It was found in all simulations that when the estimated $1/k_r$ was higher than expected, the fits were bad as sometimes indicated by the statistical tests, i.e., high χ^2_v, high z-values and bad WRES-plots, and sometimes by discrepancies between estimated and expected values of a_i and k_i. Also, a smaller value of $1/k_r$ than expected indicated that the model which was proposed and estimated was only a good mathematical description of the data when the χ^2_v and z were acceptable, but not necessarily the best phys-

ical description of the investigated system. Thus, the best χ^2_v, z, and WRES-plot do not necessarily give the best physical parameter estimates (Löfroth and Almgren 1983). In these cases k_r is suggested to be fixed at the expected value during the deconvolution. However, since this might impose restrictions on the minimization with convergence to a false minimum, the real experiments should be carried out with references with different lifetimes.

However, some significant deviations between estimated and expected values were found. First, a small difference was found in all simulations between estimated $1/k_r$ and the known input. This was mainly attributed to the fact that the time-division, 0.344 ns channel^{-1}, was too coarse to meet the requirements to estimate in some cases reference lifetimes of 0.25 ns. It has been suggested (Selinger et al. 1983) that the optimum choice of time-division is 1/20 of the expected lifetime. However, a value of 0.344 ns channel^{-1} was chosen so the generated experiments were comparable to the real, in which a compromize must be made with regards to high time resolution with consequently long data collection times. Also, instead of a true convolution integration when the data were generated, the fast convolution algorithm with discrete values of $I(t)$ was applied. This certainly introduces accumulated errors in the data.

Second, the results from one deconvolution presented in Table 1 showed severe discrepancies between expected and estimated values as well as bad statistical tests. The reference decay was in this example described by $1/k_r = 5$ ns, while the deconvoluted decay contained $1/k_1 = 2$ ns and $1/k_2 = 5$ ns. It is seen from Eq. (3b) that in this case one of the exponentials of $F_{55}(t)$ would have had zero weight and that a single exponential analysis would have sufficed. Only the facts that the expected lifetime (2 ns) was found and that the z-value was good, indicated an acceptable one component analysis. For comparison a two components analysis is shown. It was clear that the second estimated component, $1/k_r = 4.14$ ns, was insignificant, as judged by the estimated a_2 and its standard deviation. Similar results have been obtained in all situations when deconvolutions were carried out using a reference curve that decayed more slowly or with nearly the same rate as one component in the $F_{55}(t)$ curve. A plausible explanation could be that the random errors in the $F_{r,55}(t)$ pulse propagate in the iterative convolution with the result that the weighting factors, $(F_{55}(t)^{1/2})$, of WRES(i) are incorrect (Irvin et al. 1981; Zuker et al., in press), so that a standard $\chi^2{}_v$-test is inapplicable. It seems that these effects will be more pronounced in this kind of analysis than when the $F_{r,55}(t)$ pulse is fast. However, for the moment this is still a problem, as are the bad estimates of k_r.

The conclusions that were drawn from the experiments reported in Table 1 were confirmed by the fluorescence anisotropy deconvolutions. In Table 2 some of the generated decays are given, together with the results from their deconvolutions with a reference with $1/k_r = 0.23$ ns (estimated as discussed earlier).

A typical analysis started with the deconvolution of $F_{55}(t)$ alone to have good starting parameters in the global analysis of $F_{55}(t)$, $F_{pa}(t)$, and $F_{pe}(t)$ that followed. In this global analysis a_i and k_i were first fixed to estimate r_n, k_n and k_r and in the second analysis all of the parameters were estimated. If the $1/k_r$ estimate was lower than expected, it was held constant during an extra deconvolution. The analyses were not accepted until expected values of the parameters were obtained and/or the statistical tests were acceptable.

Two important conclusions were drawn. If the crossterms had been excluded in $r(t)f_{55}(t)$ when the data were generated, it was in many cases not possible to deconvolute to acceptable results, i.e., it was not possible to decide whether the crossterms had been excluded or not. However, when the total number of counts in the curves were raised, these difficulties disappeared for some of the curves. The main conclusion was that very good statistics were needed for the generated decays. For example, more than 10^5 counts seemed necessary for deconvoluting curves generated from $r(t) = 0.15\exp(-t/3.0) + 0.15\exp(-t/10.0)$ and $f_{55}(t) = 0.60\exp(-t/2.0) + 0.40\exp(-t/5.0)$ when the crossterms were excluded. This was also concluded when deconvolutions were carried out according to Eqs. (1), (8), and (9) with $I(t)$, which showed that the difficulties were not characteristic for the global-reference method.

Thus, the relatively high precision of the data in these simulated experiments was in many situations not high enough. However, in some cases the relative magnitudes of the amplitudes a_i and r_n and the decay constants k_i and k_n may replace the demand for very high number of counts in the decays. Also, one way to alleviate this problem would be to change the a_i/r_n ratios by carrying out the experiments at different excitation wavelengths, as discussed before.

It is also pertinent to mention that in most cases successful deconvolutions of the generated anisotropy curves could be attained by a global analysis of only $F_{55}(t)$ and $F_{pa}(t)$. In real experiments this is not expected due to non-random errors in the data (drift, scattered light etc.).

B. Real experiments

First the quenching experiments of PTP, PPO, POPOP, and DIMPOPOP will be discussed. The experiments aimed in the beginning at the possibility of accurately determining the lifetimes of some well characterized substances which could be used as fixed lifetimes during the analysis (Wahl et al. 1974). However, the computer-simulated experiments showed that it was preferable to use fast reference decays with varying decay constants in the global-reference deconvolutions. Therefore, the purpose of the experiments was to determine Stern-Volmer quenching constants for the systems, so that references with predictable lifetimes could easily be prepared. The results, given in Table 3, were obtained in separate experiments over a period of several months. In each experiment a quenched solution was used as $F_{r,55}(t)$ to deconvolute an unquenched solution of the same substance. Usually two to three pairs of curves were sampled and the reference decay constant, k_r, and the unquenched constant, k_0, were determined in a global analysis with both k_r and k_0 as common parameters. The experiments were often done before and after experiments on other systems, for which the quenched solutions were used as references. The results from the experiments were compiled in a plot of $k_r/k_0 - 1$ vs known [NaI].

Another approach which could have been taken was to globally analyze say 30 pairs of decays, obtained from 5 experiments at 6 different quencher concentrations. In this case, it would have been more convenient to use Eq. (3b) in a slightly rearranged form:

$$F_i^{(j)}(t) = F_{r,i}^{(j)}(t)\, a_i^{(j)} + F_{r,i}^{(j)}(t) * (a_i^{(j)}\, k_q\, C_{\mathrm{NaI}}^{(j)} \exp(-k_0 t))$$

where k_q is the Stern-Volmer quenching constant defined by $k_r^{(j)} = k_0 + k_q\, C_{\mathrm{NaI}}^{(j)}$, $j = 1, 2, \ldots, 6$ and subscript "i" refers to the 5 experiments carried out at each concentration $C_{\mathrm{NaI}}^{(j)}$.

The reported lifetimes of PTP (1.04 ns), PPO (1.47 ns), POPOP (1.25 ns), and DIMPOPOP (1.36 ns) were in good agreement with reports from other studies (Lakowicz et al. 1981). The Stern-Volmer constants (7.65×10^9, 4.62×10^9, 5.94×10^9 and $3.72 \times 10^9\, M^{-1}\, s^{-1}$) were reliable, being near diffusion-controlled. The plots of $k_r/k_0 - 1$ vs concentration were linear, but the *steady-state* plots were somewhat curved upward, most of the effect however being attributed to the fact iodide absorption contributed to the absorption of excitation light. Part of the curvature is due to the transient-effect, discussed in detail by Ware et al. (Nemzek and Ware 1975; Ware and André 1983). This effect might be described by a $\sqrt{t}$ dependence in the decay: $f(t) = f(0) \exp(-a t) \exp(-b \sqrt{t})$, where a and b in the simplest theory are functions of k_0, R (the encounter distance), D (the sum of the diffusion coefficients) and the quencher concentration. Reasonable estimates relevant for the present study are $k_0 = 1/1.25\ \mathrm{ns}^{-1}$, $R = 3$ Å, $D = 3 \times 10^{-9}\ \mathrm{m^2\, s^{-1}}$, and $[\mathrm{NaI}] = 0.6\, M$, giving $k_q/k_0 = 5.45\, M^{-1}$. Then $a = 4.47\ \mathrm{ns}^{-1}$ and $b = 0.644\ \mathrm{ns}^{-1/2}$, which means that the transient term would not be detectable for times $> 50-75$ ps. It might be argued that the transient term in fact is convoluted with $I(t)$ and that this might influence the deconvolutions. However, in the last four examples of Table 1, results are presented from simulations to investigate the transient effect. $I(t) * \exp(-t/1.25)$ was first deconvoluted with $I(t) * \exp(-t/0.22)$ and $I(t) * \exp(-a t - b \sqrt{t})$ according to Eq. (3a) to estimate the k_r's. In a second simulation,

$$I(t) * (0.80 \exp(-t/1.25) + 0.20 \exp(-t/5.00))$$

was first analyzed in deconvolutions with estimation of the k_r's. In a second analysis the k_r's were fixed at the values previously found in the deconvolutions of $I(t) * \exp(-t/1.25)$. It is seen that there is no indication of worse fits when the transient decay was used. These results, and the fact that in our experiments the leading part of the decays are fitted, show that, within the precision of the measurements, the transient effect had not significantly disturbed the analyses. Higher concentrations of NaI than those giving quenched reference lifetimes of about 0.25 ns were not used in order not to have the lifetime much shorter than the time-division in the experiments. The reported values of k_q/k_0 and k_0, Table 3, were then accepted and have been used for guidance in other experiments to judge whether a deconvolution was reliable or not, as discussed in connection with the results from the simulated experiments.

The choice of substances investigated in this study was partly dictated by the work in progress in our laboratory. Thus, PTP is a suitable reference for studies of the fluorescence of tryptophan in proteins. Although Trp is modified when it is part of a protein, an understanding of its photophysics will in any case be of considerable value. The molecule has

Table 3. Stern-Volmer parameters for the quenching of PTP, PPO, POPOP, and DIMPOPOP in ethanol by NaI. Not degassed solutions

	$k_q/k_0/M^{-1}$	$1/k_0$/ns	$[\mathrm{NaI}]_{\max}/M$
PTP	7.960 ± 0.310	1.04 ± 0.04	0.5
PPO	6.793 ± 0.322	1.47 ± 0.02	0.65
POPOP	7.419 ± 0.184	1.25 ± 0.03	0.5
DIMPOPOP	5.054 ± 0.058	1.36 ± 0.02	0.85

Table 4. Fluorescence lifetimes and amplitudes at different wavelengths. Results from experiments on Trp in a 0.1 *M* potassium phosphate buffer, pH = 7.1, 20 °C. Deconvolutions with quenched PTP (expected lifetime = 0.29 ns estimated = 0.30 ns). For comparison: results from experiments on a mixture of POPOP, anthracene, and DPA in ethanol. Deconvolution with quenched POPOP (expected lifetime = 0.25 ns, estimated = 0.22 ns)[a]

Trp								
Emission wavelength/nm	325	335	345	355	365	375	385	common $1/k_0$/ns
a_1	0.293 ± 0.145	0.263 ± 0.158	0.225 ± 0.197	0.161 ± 0.167	0.129 ± 0.146	0.092 ± 0.233	0.056 ± 0.161	0.67 ± 0.19
a_2	0.702 ± 0.041	0.730 ± 0.041	0.767 ± 0.045	0.829 ± 0.040	0.857 ± 0.041	0.880 ± 0.054	0.892 ± 0.044	3.14 ± 0.04
a_3	0.005 ± 0.014	0.007 ± 0.014	0.008 ± 0.015	0.009 ± 0.014	0.014 ± 0.014	0.029 ± 0.015	0.052 ± 0.017	7.79 ± 1.21
χ^2_v	1.09	1.06	0.89	1.28	1.39	1.31	1.19	
z	1.71	0.55	0.44	0.93	0.03	0.59	2.68	

POPOP + anthracene + DPA					
Emission wavelength/nm	399	418	450	500	common $1/k_0$/ns
a_1	0.548 ± 0.074	0.683 ± 0.064	0.774 ± 0.055	0.864 ± 0.055	1.26 ± 0.04[c]
%[b]	27.1 (27.6)	34.9 (39.0)	43.8 (43.6)	58.5 (57.3	
a_2	0.271 ± 0.024	0.157 ± 0.022	0.058 ± 0.020	0.026 ± 0.016	4.07 ± 0.23[c]
%[b]	40.5 (43.8)	25.8 (25.2)	10.6 (17.0)	5.7 (6.7)	
a_3	0.145 ± 0.015	0.160 ± 0.014	0.167 ± 0.013	0.110 ± 0.010	6.08 ± 0.19[c]
%[b]	32.4 (28.6)	39.3 (35.8)	45.6 (39.4)	35.8 (36.0)	

[a] The results were obtained when k_r was fixed at the expected value. The results were not significantly different when k_r was estimated during the analysis

[b] These are the relative contributions to the total steady-state intensity. The first number was calculated as $a_i/k_i/\Sigma\,(a_i/k_i)$ (ground state heterogeneity), while the second number was calculated from known volume fractions and individual spectra of the stock solutions

[c] Individual analyses of data of the stock solutions gave lifetimes of 1.25 ns (POPOP), 4.13 ns (anthracene), and 6.04 ns (DPA)

been investigated in numerous recent studies (Petrich et al. 1983 and references therein), and in this report only the results, Table 4, of one study of Trp in buffer are given. However, it is the first study that has taken advantage of the global analysis technique to analyze this system. The fluorescence was sampled at 7 different wavelengths and deconvoluted with a quenched PTP solution (expected lifetime = 0.29 ns). When the decays were analyzed individually, which incidentally, it must be emphasized, is always done on individual curves, two components described the data satisfactory. The lifetimes at the different wavelengths were essentially the same except for the two longest lifetimes. In the global analysis it was however necessary to use three components to describe the data. Noteworthy were the large standard deviations for the a_i of the fast and slow decays. The estimated lifetimes agreed with one other report on this system (Gudgin et al. 1981). However, the wavelength dependence in a_i and the number of exponentials are still under discussion. Different conformers of the indole ring undergoing slow intramolecular conversions have been reported (Szabo and Rayner 1980), while other investigations (Petrich et al. 1983) report that charge transfer effects are essential to explain the non-exponential behaviour of Trp. Thus it seems that further experiments are needed on Trp in solution and that these studies should be carried out using the global-reference method presented here. Deconvolutions could then be carried out assuming also, for example, non-sumexponential behaviour of the decays.

The ability of the method presented in this work to resolve the decays into their true components are shown in Table 4 for comparison with the Trp study. Separate two component analyses at each wavelength of a mixture of POPOP ($1/k_0 = 1.25$ ns), anthracene ($1/k_0 = 4.13$ ns), and DPA ($1/k_0 = 6.04$ ns) in ethanol (the individual lifetimes determined separately with quenched POPOP as reference) were statistically acceptable, but the lifetimes changed with the emission wavelength. When the three-component global analysis was carried out, the three

Table 5. Fluorescence anisotropy parameters from experiments on holo-stellacyanin and apo-stellacyanin in 0.1 *M* potassium phosphate buffer, pH = 7.1, 20 °C; deconvolutions with quenched PTP (expected lifetime = 0.31 ns). For comparison: results from experiments on POPOP and DPA in paraffin oil at 20 °C; deconvolutions with quenched POPOP (expected lifetime = 0.27 ns). Decay times are in nanoseconds

	$\chi^2_{\nu_{55}}$	z_{55}	$\chi^2_{\nu pa}$	z_{pa}	$\chi^2_{\nu pe}$	z_{pe}
Holo-stellacyanin						
$f_{55}(t) = 0.74 \exp(-t/1.52) + 0.26 \exp(-t/3.68)$ $\pm 0.05 \quad \pm 0.06 \pm 0.02 \quad \pm 0.12$	0.97	0.83[a]				
$r(t) = 0.17 \exp(-t/6.1)$ $\pm 0.02 \quad \pm 1.8$	0.89	0.58	1.96	0.37	1.40	1.85
$r(t) = 0.15 \exp(-t/8.1) + 0.09 \exp(-t/^b)$ $\pm 0.02 \quad \pm 4.4 \pm 0.15$	1.11	0.37	1.33	0.87	1.24	0.24
Apo-stellacyanin						
$f_{55}(t) = 0.28 \exp(-t/1.23) + 0.71 \exp(-t/3.44) + 0.01 \exp(-t/9.40)$ $\pm 0.07 \quad \pm 0.21 \pm 0.03 \quad \pm 0.07 \pm 0.008 \quad \pm 2.76$	1.24	1.22[a]				
$r(t) = 0.14 \exp(-t/7.7)$ $\pm 0.01 \quad \pm 2.1$	1.39	0.82	2.01	3.69	1.61	2.88
$r(t) = 0.13 \exp(-t/8.7) + 0.13 \exp(-t/^b)$ $\pm 0.01 \quad \pm 2.9 \pm 0.25$	1.25	0.39	1.51	1.78	1.46	0.30
DPA						
$f_{55}(t) = 1.00 \exp(-t/7.01)$, $f_r(t) = 1.00 \exp(-t/0.23)$ $\pm 0.02 \quad \pm 0.09 \quad \pm 0.02 \quad \pm 0.01$	1.21	0.16[a]				
$r(t) = 0.25 \exp(-t/5.4)$ $\pm 0.02 \quad \pm 1.0$	1.43	0.68	0.97	2.17		
POPOP						
$f_{55}(t) = 1.00 \exp(-t/1.07)$, $f_r(t) = 1.00 \exp(-t/0.25)$ $\pm 0.02 \quad \pm 0.02 \quad \pm 0.02 \quad \pm 0.01$	1.16	1.34[a]				
$r(t) = 0.36 \exp(-t/8.4)$ $\pm 0.02 \quad \pm 3.4$	1.17	1.42	1.12	0.13		

[a] These results were obtained from individual analyses
[b] $\Phi < 0.2$ ns when fixed in the analysis with the crossterms included

decay constants and their a_i were recovered. It is worth noticing that the small amount (6.7%) of the anthracene fluorescence at 500 nm, determined from known volume fractions and individual steady-state spectra, was present in measurements with only 10^4 counts in the maxima of the curves. Even fewer counts in the decays (10^3 at the maxima) have been used in studies of substituted bisanthrylalkanes. One studied system shows three emitting species in excited state reactions. From observed and globally analyzed decays, sampled at every third to fifth nanometer between 400 nm and 570 nm, it has been possible to derive the species associated spectra, although the fluorescence of these individual spectra overlap strongly (Löfroth 1985 b, c). Such deconvolutions are not possible without careful considerations of the wavelength-dependent transit-time effects.

Fluorescence anisotropy measurements are a powerful tool with which to study conformational changes of proteins. The protein stellacyanin, SC, is a single copper-containing glycoprotein of low molecular weight ($M = 20{,}000$) containing three tryptophan residues. In recent studies (Dahlin et al. 1984) the self exchange rate (rate of the reaction Cu(II) ⇄ Cu(I)) of SC was determined by e.p.r. methods. In current work, SC with Ni(II) and Co(II) substituted for Cu(II) has been studied with NMR (Reinhammar et al., in preparation). It was therefore of interest to see if these substitutions were reflected in the fluorescence anisotropy of the modified protein. The results so far obtained are reported in Table 5.

The fluorescence intensity decay at 369 nm of holo-SC could be described by two lifetimes, while three components were necessary for the apo-SC. The different qualities were also reflected in the steady-state spectra: the apo-form showing a slightly higher intensity for wavelengths above 350 nm, while the maxima (325 nm) were the same for the spectra. Further experiments, i.e., fluorescence quenching with different quenchers, are needed to explain the physical origin of the different lifetimes. However, without going into details about the photophysics, it was possible to describe the anisotropies phenom-

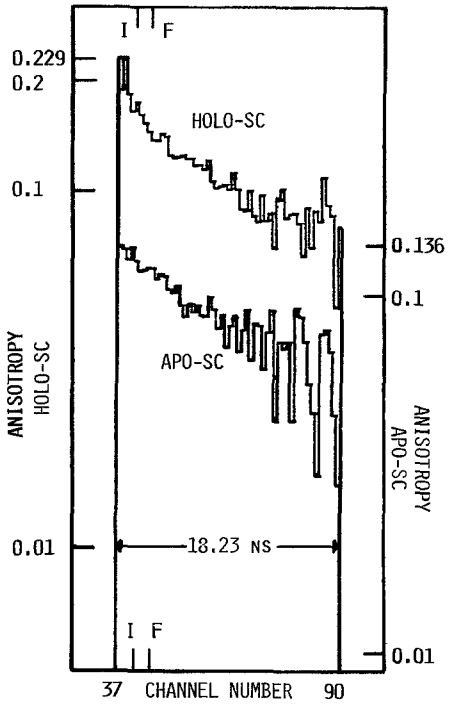

Fig. 2. "Pseudo-anisotropies" of Stellacyanin. Upper: holo-protein, Lower: apo-protein. The curves have been vertically displaced for the sake of clearness and truncated due to the scatter in the data. Time division: 0.345 ns channel^{-1}. I at channel 41 and F at channel 45 indicates the position of the peak of a scattered decay $I(t)$ and of the fluorescence decays respectively

enologically. From the "pseudo-anisotropies" calculated according to Eq. (5) it is seen, Fig. 2, that the anisotropy of the holo-protein seemed non-exponential, while the apo-SC seemed to decay with a single exponential. (The data in Fig. 2 were truncated before channel 37 and after channel 90 due to the scattering of the data.) However, it must be emphasized that these plots do not show the real behaviour of the anisotropy, a fact revealed by the deconvolutions. One-component analyses gave $r(0)$ values of 0.17 (holo) and 0.14 (apo), which were much lower than expected (~ 0.20) for tryptophan in proteins excited at 295 nm. Two-component analyses, which were possible only with fixed values of k_i, showed that both the anisotropies were better described by at least two exponentials, Table 5. The fast one had $1/k_n < 0.2$ ns and contributed more to the decay of the apo-protein. The slow decays were approximately the same. The uncertainty in these estimations was attributed mainly to too coarse a time-division and too small a number of counts in the decays. Nevertheless, at this stage of the investigation a reasonable overall explanation of the fluorescence intensity curves, the steady-state spectra and the anisotropy decays could be that one or more of the tryptophans are exposed to less hydrophobic environments and gain a higher degree of rotational freedom when the copper is removed.

A test of the reliability of these anisotropy experiments is also reported in Table 5. POPOP and DPA in paraffin oil were chosen as they were assumed to behave in a predictable way. The results showed that DPA behave like an isotropic rotator. The estimated $r(0)$, 0.25, was somewhat lower than was found from a steady-state Perrin plot ($r(0) = 0.288$) when it was excited at 365 nm. This might indicate substantial vibronic coupling in the excited state, or a mixture of states. The $r(0)$ value found for POPOP was smaller than the theoretical 0.4. This could be the result of non-parallel transition moments in absorption and emission, or of a fast decay which could not be resolved with our instrument. The shape of the POPOP molecule (rodlike) suggests that the second alternative might be realistic. Also, it was found that the $F_{pa}(t)$ could not be resolved into the two components expected for isotropic rotation of a homogeneous emitting species. More studies of this molecule with excitation at other wavelengths and deconvolution with global analysis would be of interest.

Concluding remarks

A method has been presented for deconvolution of fluorescence intensity and anisotropy decays sampled with the single-photon-counting technique. The methods combines

a) a reference method (Wahl et al. 1974; Wahl 1979; Gaudochon and Wahl 1978), which was extended and based on quenched references, and
b) global analysis of the data (Knutson et al. 1983).

The method relies on finding references that decay with single exponentials. The compounds that were investigated and chosen as references were characterized, within the precision of the measurements, by single exponential decays and showed fluorescence from 325 nm to 550 nm with excitation from below 300 nm up to 400 nm. Reports and studies of other suitable references should be of the utmost importance, since it is decisive for correct interpretation of decay data that the data are as far as possible free from artifacts. In the studies the advantages of global analysis should be born in mind. It has been demonstrated that straightforward accurate and reliable deconvolutions of fluorescence intensity and fluorescence anisotropy decay data are possible with the global-reference method.

Acknowledgements. The author gratefully acknowledge valuable comments and suggestions given by one of the referees. This work was financially supported by grants from the Swedish Natural Science Research Council.

Appendix

The general form of Eq. (3b) has been presented earlier (Wijnaendts van Resandt et al. 1982; Zuker et al., in press):

$$F(t) = F_r(t) f(0) + F_r(t) * X(t)$$

where (A3a)

$$X(t) = k_r f(t) + \frac{\mathrm{d}}{\mathrm{d}t} f(t) .$$

For use in connection with global analysis of decay curves from different experiments, j, and for applications in fluorescence anisotropy experiments, the general algorithms are presented in this paper:

$$F^{(j)}(t) = F_r^{(j)}(t) f^{(j)}(0) + F_r^{(j)}(t) * X^{(j)}(t) ,$$

where (A3b)

$$X^{(j)}(t) = k_r^{(j)} f^{(j)}(t) + \frac{\mathrm{d}}{\mathrm{d}t} f^{(j)}(t) ,$$

and where $k_r^{(j)}$ can be one of the common parameters in the experiments, as in this study.

Also, the general forms of Eqs. (10a) and (10b) are given by

$$F_{\mathrm{pa}}^{(j)}(t) = F_r^{(j)}(t) f_{\mathrm{pa}}^{(j)}(0) + F_r^{(j)}(t) * X_{\mathrm{pa}}^{(j)}(t) ,$$

where

$$f_{\mathrm{pa}}^{(j)}(0) = \tfrac{1}{3} f_{55}^{(j)}(0) \{2 r^{(j)}(0) + 1\} \quad \text{(A10a)}$$

and

$$X_{\mathrm{pa}}^{(j)}(t) = \tfrac{1}{3} f_{55}^{(j)}(t) \left\{2 k_r^{(j)} r^{(j)}(t) + k_r^{(j)} + 2 \frac{\mathrm{d}}{\mathrm{d}t} r^{(j)}(t)\right\} + \tfrac{1}{3} \{2 r^{(j)}(t) + 1\} \frac{\mathrm{d}}{\mathrm{d}t} f_{55}^{(j)}(t) ,$$

and for the perpendicular component

$$F_{\mathrm{pe}}^{(j)}(t) = F_r^{(j)}(t) f_{\mathrm{pe}}^{(j)}(0) + F_r^{(j)}(t) * X_{\mathrm{pe}}^{(j)}(t)$$

where

$$f_{\mathrm{pe}}^{(j)}(0) = \tfrac{1}{3} f_{55}^{(j)}(0) \{1 - r^{(j)}(0)\} \quad \text{(A10b)}$$

and

$$X_{\mathrm{pe}}^{(j)}(t) = \tfrac{1}{3} f_{55}^{(j)}(t) \left\{k_r^{(j)} - k_r^{(j)} r^{(j)}(t) - \frac{\mathrm{d}}{\mathrm{d}t} r^{(j)}(t)\right\} + \tfrac{1}{3} \{1 - r^{(j)}(t)\} \frac{\mathrm{d}}{\mathrm{d}t} f_{55}^{(j)}(t) .$$

For $F_{55}^{(j)}(t)$ Eq. (A3b) applies.

References

Almgren M (1974) Analysis of pulse fluorometry data of complex systems. Ph.D. Thesis, Chalmers University of Technology, Göteborg

Almgren M, Löfroth J-E (1982) Effects of polydispersity on fluorescence quenching in micelles. J Chem Phys 76:2734–2742

Birch DJS, Imhof RE (1982) The origin of fluorescence from trans-trans diphenylbutadiene. Chem Phys Lett 88:243–247

Dahlin S, Reinhammar B, Wilson M (1984) Direct measurements of the self-exchange rate of stellacyanin by a novel e.p.r. method. Biochem J 218:609–614

Ehrenberg M, Rigler R, Wintermeyer W (1979) On the structure and conformational dynamics of yeast phenylalanine-accepting transfer ribonucleic acid in solution. Biochemistry 18:4588–4599

Gaudochon P, Wahl Ph (1978) Pulsefluorimetry of tyrosyl peptides. Biophys Chem 8:87–104

Gilbert CW (1983) A vector method for the non-linear least squares reconvolution-and-fitting analysis of polarized fluorescence decay data. In: Cundall RB, Dale RE (eds) Time-resolved fluorescence spectroscopy in biochemistry and biology. NATO ASI, St. Andrews, Scotland. Plenum Press, New York, pp 605–606

Grinvald A, Steinberg IZ (1974) On the analysis of fluorescence decay kinetics by the method of least-squares. Anal Biochem 59:583–598

Gudgin E, Lopez-Delgado R, Ware WR (1981) The trytophan fluorescence lifetime puzzle. A study of decay times in aqueous solution as function of pH and buffer composition. Can J Chem 59:1037–1044

Helman WP (1971) Analysis of very fast transient luminescence behavior. Int J Radiat Phys Chem 3:283–294

Irvin JA, Quickenden TI, Sangster DF (1981) Criterion of godness of fit for deconvolution calculations. Rev Sci Instrum 52:191–194

Isenberg I (1975) Time decay fluorometry by photon counting. In: Chen RF, Edelhoch H (eds) Biochemical Fluorescence: concepts. Marcel Dekker, New York, pp 43–77

Knight AEW, Selinger BK (1971) The deconvolution of fluorescence decay curves. A non-method for real data. Spectrochim Acta 27A:1223–1234

Knight AEW, Selinger BK (1973) Single photon decay spectroscopy. Aust J Chem 26:1–27

Knutson JR, Beechem J, Brand L (1983) Simultaneous analysis of multiple fluorescence decay curves: a global approach. Chem Phys Lett 102:501–507

Lakowicz JR, Balter A (1982) Resolution of initially excited and relaxed states of tryptophan fluorescence by differential-wavelength deconvolution of time-resolved fluorescence decays. Biophys Chem 15:353–360

Lakowicz JR, Cherek H, Balter A (1981) Correction of timing errors in photomultiplier tubes used in phase-modulation fluorometry. J Biochem Biophys Methods 5:131–146

Lewis C, Ware WR, Doemeny LJ, Nemzek TL (1973) The measurement of short-lived fluorescence decay using the single photon counting method. Rev Sci Instrum 44:107–114

Libertini LJ, Small EW (1984) F/F deconvolution of fluorescence decay data. Anal Biochem 138:314–318

Löfroth JE (1982) Fluorescence quenching in micelle solutions. Ph.D. Thesis, University of Göteborg, Göteborg

Löfroth JE (1985a) Deconvolution of single photon counting data with a reference method and global analysis. In: Szabo AG, Masotti L (eds) Excited state probes in biochemistry and biology. NATO ASI, Acireale, Italy. Plenum Press, New York (in press)

Löfroth JE (1985b) TRES, DAS, and SAS (Time-resolved emission spectra, decay associated spectra, and species associated spectra). Application to excited state reactions. J Phys Chem (submitted for publication)

Löfroth JE (1985c) Recent developments in the analysis of fluorescence intensity and anisotropy data. (submitted for publication in an upcoming special issue of *Analytical Instrumentation* on Time Resolved Fluorescence Spectroscopy)

Löfroth JE, Almgren M (1982) Quenching of pyrene fluorescence by alkyl iodides in sodium dodecyl sulphate micelles. J Phys Chem 86:1636–1641

McKinnon AE, Szabo AG, Miller DR (1977) The deconvolution of photoluminescence data. J Phys Chem 81:1564–1570

Nemzek TL, Ware WR (1975) Kinetics of diffusion-controlled reactions: Transient effects in fluorescence quenching. J Chem Phys 62:477–489

Petrich JW, Chang MC, McDonald DB, Fleming GR (1983) On the origin of nonexponential fluorescence decay in tryptophan and its derivatives. J Am Chem Soc 105:3824–3832

Rayner DM, McKinnon AE, Szabo AG (1976) Confidence in fluorescence lifetime determinations: a ratio correction for the photomultiplier time response variation with wavelength. Can J Chem 54:3246–3259

Rayner DM, McKinnon AE, Szabo AG (1977) Correction of instrumental time response variation with wavelength in fluorescence lifetime determinations in the ultraviolet region. Rev Sci Instrum 48:1050–1054

Reinhammar B (1970) Purification and properties of laccase and stellacyanin from Rhus Vernicifera. Biochim Biophys Acta 205:35–47

Selinger BK, Hinde AL (1983) Least squares methods of analysis. I. Confidence limits. In: Cundall RB, Dale RE (eds) Time-resolved fluorescence spectroscopy in biochemistry and biology. NATO ASI, St. Andrews, Scotland. Plenum Press, New York, pp 129–141

Selinger BK, Harris C, Kallir K (1983) Least squares methods of analysis. II. Convolution and data optimization. In: Cundall RB, Dale RE (eds) Time-resolved fluorescence spectroscopy in biochemistry and biology. NATO ASI, St. Andrews, Scotland. Plenum Press, New York, pp. 143–153

Szabo AG, Rayner DM (1980) Fluorescence decay of tryptophan conformers in aqueous solution. J Am Chem Soc 102:554–563

Valeur B (1978) Analysis of time-dependent fluorescence experiments by the method of modulating functions with special attention to pulse fluorometry. Chem Phys 30:85–93

Wahl Ph (1977) Statistical accuracy of rotational correlation times determined by the photocounting pulse fluorimetry. Chem Phys 22:245–256

Wahl Ph (1979) Analysis of fluorescence anisotropy decays by a least square method. Biophys Chem 10:91–104

Wahl Ph, Auchet JC, Donzel B (1974) The wavelength dependence of the response of a pulse fluorometer using the single photoelectron counting method. Rev Sci Instrum 45:28–32

Ware WR (1971) Transient luminescence measurements. In: Lamola AA (ed) Creation and detection of the excited state, Vol 1, part A. Marcel Dekker, New York, pp 213–302

Ware WR, André JC (1983) The influence of diffusion on fluorescence quenching. In: Cundall RB, Dale RE (eds) Time-resolved fluorescence spectroscopy in biochemistry and biology. NATO ASI, St. Andrews, Scotland. Plenum Press, New York, pp 363–392

Ware WR, Doemeny LJ, Nemzek TL (1973) Deconvolution of fluorescence and phosphorescence decay curves. A least square method. J Phys Chem 77:2038–2048

Ware WR, Pratinidhi M, Bauer RK (1983) Performance characteristics of a small side-window photomultiplier in laser single-photon fluorescence decay measurements. Rev Sci Instrum 54:1148–1156

Wijnaendts van Resandt RW, Vogel RH, Provencher SW (1982) Double beam fluorescence lifetime spectrometer with subnanosecond resolution: Application to aqueous tryptophan. Rev Sci Instrum 53:1392–1397

Zuker M, Szabo AG, Krajcarski DT, Selinger BK (in press) Correction methods in TCPC & multicomponent analysis. In: Szabo AG, Masotti L (eds) Excited state probes in biochemistry and biology. NATO ASI, Acireale, Italy. Plenum Press, New York